JOURNAL OF NANO- AND ELECTRONIC PHYSICS
Vol. **10** No 4, 04005(5pp) (2018)

ЖУРНАЛ НАНО- ТА ЕЛЕКТРОННОЇ ФІЗИКИ
Том **10** № 4, 04005(5cc) (2018)

Kinetics of Blue Emission during Ultraviolet Insolation on Germanosilicate Optical Fiber

H. Kuswanto[1,*], F. Goutaland[2], A. Boukenter[2], Y. Ouerdane[2]

[1] *Universitas Negeri Yogyakarta, Yogyakarta, Indonesia*
[2] *Laboratoire Traitement du Signal et Instrumentation UMR CNRS 5516*
Université Jean Monnet de Saint Etienne, France

(Received 06 February 2018; revised manuscript received 12 August 2018; published online 25 August 2018)

The research aimed to study the kinetics of 400 nm blue emission during ultraviolet insolation on germanoslicate optical fiber, hydrogenated, and non-hydrogenataed. The hydrogenation of the fibers was carried out at room temperature under 150 atm for 4 weeks. The focused frequency doubled Argon laser ultraviolet beams were directed to the core of the unsheathed fiber. The light beams emerging from the end of the fiber were directed towards a detector. Kinetics the creation of defects in the hydrogenated fiber followed the power law for low-fluency insolation. At high fluency, the formation of defects followed the principle of two photosensitization or serial steps.

Keywords: Blue, Emission, Ultraviolet, Optical Fiber, Hydrogen

DOI: 10.21272/jnep.10(4).04005

PACS numbers: 42.81.Dp, 61.80.Ba, 85.40.Ry, 68.60.Dv

1. INTRODUCTION

Study in the defects of fibers and glasses based on germanium-doped silica have grown due to its ability to be photoinduced by ultraviolet (UV) light. This character might be exhibit the second harmonic generation [1] and refractive-index gratings [2-7]. Hydrogen loading has been used to increase the photosensitivity [3].

The defects which are involved is interesting study to elucidate. The conversion of the Germanium lone pair center (GLPC) into GeE' centers is based on non-hydrogenataed fiber [4]. However, in hydrogenated fiber GeH obtained from UV-induced reactions of H_2 and GeO_2 are mainly generated from GeE' centers [5].

The blue emission is generated both with 325 nm excitation at the T1 level and at 244 nm in the S1 level of the oxygen deficient centers (ODC) defects [6]. Absorption related to these levels has been extensively studied since its bleaching leads to a variation of the refractive index exploited for the photo-inscription of Bragg gratings [7]. However, the results relating to the evolution of the emission associated with it remain controversial. For example, it did not observe a significant variation (less than 2%) during insolation by a pulsed laser of a germanosilicate fiber at 242 nm (15 ns, 25 Hz) for 5 minutes with energy densities of the order of 200 mJ/cm^2/pulse [8]. Other authors have shown that this emission undergoes a decrease during the insolation [9-10]. For this reason, we decided to follow the evolution of this emission in our fibers.

The transformation of the centers at the origin of this emission is accompanied by a modification of the refractive index and is involved in the photosensitivity of the germanosilicates fibers. The emission evolution at 400 nm is discussed as part of a two-stage transformation of the transmitting centers as proposed [11]. The discussion of the results showed that this model does not make it possible to account for all of our experimental observations. In the light of this discussion, we propose a modification of this model and an allocation of the products of the various transformation stages of the transmitting centers around 400 nm.

2. EXPERIMENTAL SET-UP

This study focused on a Corning standard germanosilicate fiber. The core diameter of 9 μm, a difference in core-cladding refractive index of $4.5 \cdot 10^{-3}$ and a germanium concentration of 4.8%. The fiber is monomode at 1330 nm and 1550 nm and is intended for telecommunication applications. Chemical stripping is conducted towards the jacket of the fiber.

The fiber hydrogenation is generally carried out under high hydrogen pressure (100 to 200 atmospheres) and at a temperature of up to 100 degrees. In our case, it was carried out at room temperature under 150 atm for 4 weeks.

To study the evolution of emission during insolation of the ultraviolet laser fiber was placed on top of a bench. Length of the fiber between the two magnets is 10 cm, of which, between a magnet and the end of the fiber towards detector is 15 cm. The focused frequency doubled Argon laser ultraviolet beams (P = 60 mW, at 244 nm) were directed to the core of the unsheathed fiber. We have used sperical and cylindrical lens. The light beams emerging from the end of the fiber were directed towards a detector. We used a double monochromator (two 1800 1/mm gratings which are identical, Jobin-Yvon HRD1) in concurrence with a GaAs photomultiplier (Hamamatsu R-943-02) equipped with a counting system. The monochromator has been programmed to detect only the wavelength at 400 nm. The computer has been reporting data every second.

We used two different lenses: cylindrical (f = 20 cm) and spherical (f = 15 cm). In one case of the cylindrical lens, we used the frequency generator to scan beams to help it from a mirror, so we can vary the length of the beams on the fiber by varying the amplitude of the scanner. The position of the beams was on the fiber to be monitored using the diffractions at the back of the

* herukus61@uny.ac.id

fiber.

The experiment was carried out for both hydrogenated and non-hydrogenated fibers for different densities of insolation power. Practically, the fiber has been placed in the focal plane of a cylindrical lens which receives the laser beam at 244 nm, via a vibrating mirror which allows, by scanning, the exposure of the fiber to a variable length. The fiber is held in the UV beam field for the duration of the experiment.

3. RESULTS AND DISCUSSION

Figure 1 shows the time evolution of the emission around 400 nm during the insolation. Insolation is performed over a length of 5 to 35 mm always at the same scanning frequency and with the same laser power at 244 nm (60 mW). In the case of the hydrogenated fiber, and for the two irradiated lengths (Figure 1.b and 1.c), there is a rapid decrease of this emission as a function of time, while it remains almost constant in the case of the non-hydrogenated fiber (Figure 1a). The kinetics of decay depend on the power density, the greater the latter, and the faster the decay. Moreover, in the case of 5 mm scanning (higher power density), the emission growth starts beyond 2500 seconds of insolation.

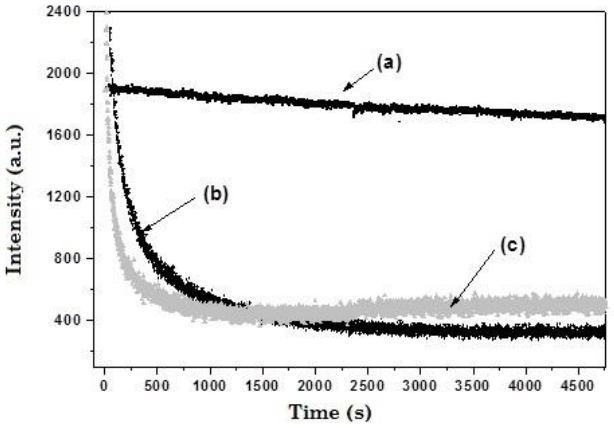

Fig. 1 – Time evolution of the emission at 400 nm under lateral insolation of 60 mW at 244 nm: (a) non-hydrogenated fiber irradiated over a length of 35 mm; (b) hydrogenated fiber irradiated over a length of 35 mm; (c) hydrogenated fiber irradiated over a length of 5 mm

In order to observe the process as a whole and to avoid lengthening the observation time, the cylindrical lens has been replaced by a spherical lens and the scanning removed, which has the effect of increasing the energy density. Figure 2 shows, under these conditions, the evolution of the emission around 400 nm in the case of the two fibers, hydrogenated and non-hydrogenated. We thus see that we are dealing with radically different kinetics. While for the non-hydrogenated fiber there is a monotonous evolution, the emission of the hydrogenated fiber shows an increase of the signal at 400 nm followed by a decrease. The monitoring of the behavior of the hydrogenated fiber as a function of the energy density shows that the phase of growth of the signal is preceded by a first phase during which the signal undergoes decay much faster than observed after the passage through the maximum. This first phase lasts in the case of Figure 2 less than a second and it is observed, with much lower energy densities, in Figure 1.

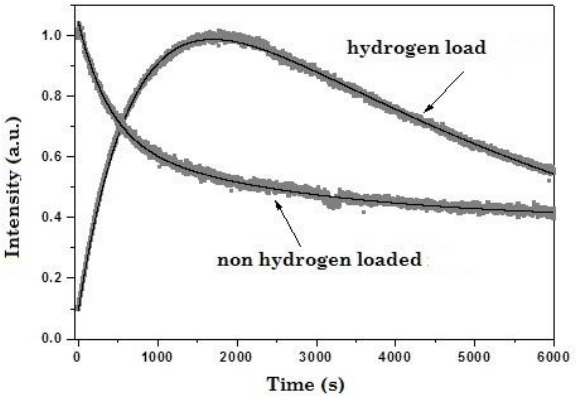

Fig. 2 – Temporal evolution of the emission at 400 nm under one 60 mW UV lateral insolation focused on the fiber. Solid lines correspond to the adjustment obtained via the model described below

Such behavior of the hydrogenated fiber could be explained by the existence of two competitive mechanisms leading, one to the destruction of the species responsible for the emission around 400 nm and the other to the creation of a species, emitting in this spectral range. This schema is reminiscent of a model to account for the contribution of color centers to variation in refractive index [11].

It is considered that the species created is none other than the destroyed species but whose formation kinetics is much slower than that of destruction. Specifically, GLPC defects, emitting around 400 nm, are defects that exist in the germanosilicates fibers prior to any treatment and that can also be generated by UV insolation. If species A is the precursor at the origin of the formation, under UV insolation and in the presence of hydrogen, of the GLPCs constituting species B which in turn is transformed into a species C, we can write the reactions (1)

$$A \xrightarrow[k]{} B \xrightarrow[k]{} C \tag{1}$$

that,

$$\frac{d}{dt}[A] = -k_1[A], \tag{2}$$

$$\frac{d}{dt}[B] = k_1[A] - k_2[B], \tag{3}$$

$$\frac{d}{dt}[C] = k_2[B] \tag{4}$$

with $[X]$ is the concentration of the species X and k_1, k_2 the constants governing the kinetics of the reactions $A \rightarrow B$ and $B \rightarrow C$ respectively. If $[X]_0$ is the concentration of the species X at the initial moment $t = 0$ and $[X]_t$ that at the instant t, we obtain:

$$[A]_t = [A]_0 e^{-k_1 t} \tag{5}$$

leading us to the following differential equation:

$$\frac{d}{dt}[B] = k_1[A]_0 e^{-k_1 t} - k_2[B], \quad (6)$$

whose solution is of the form:

$$[B] = [B_1]e^{-k_1 t} + [B_2]e^{-k_1 t}, \quad (7)$$

where $[B_1]$ and $[B_2]$ are integration constants determined according to the initial conditions. By replacing in equation (6) we get:

$$-k_2[B_1]e^{-k_2 t} - k_1[B_2]e^{-k_1 t} + k_2[B_1]e^{-k_2 t} + k_2[B_2]e^{-k_1 t} = k_1[A]_0 e^{-k_1 t}. \quad (8)$$

Giving $t = 0$,

$$-k_1[B_2] + k_2[B_2] = k_1[A]_0, \quad [B_2] = \frac{k_1}{k_2 - k_1}[A]_0. \quad (9)$$

As the very fast kinetics of destruction of species B, we can consider that its concentration is zero at the initial moment. Moreover, in Figure 2 shows that the emission around 400 nm is zero at $t = 0$, indicating the absence of sending centers at the beginning. This condition leads to:

$$[B]_{t=0} = 0 \Rightarrow B_1 + B_2 = 0 \Rightarrow [B_1] = -[B_2], \quad (10)$$

and an emission species concentration that varies with time according to the law:

$$[B]_t = \frac{k_1}{k_2 - k_1}[A]_0 \left\{e^{-k_1 t} - e^{-k_2 t}\right\}, \quad (11)$$

Under these conditions we obtain for species C the following evolutionary equation:

$$\frac{d}{dt}[C] = k_2[B] = k_2 \frac{k_1}{k_2 - k_1}[A]_0 \left\{e^{-k_1 t} - e^{-k_2 t}\right\}, \quad (12)$$

whose solution is of the form:

$$[C] = \frac{k_2}{k_2 - k_1}[A]_0(-e^{-k_1 t}) + \frac{k_1}{k_2 - k_1}[A]_0(e^{-k_1 t}) + Cte \quad (13)$$

and taking into account that the initial concentration of C is zero, we obtain:

$$[C]_{t=0} = 0 \Rightarrow Cte = +[A]_0, \quad (14)$$

$$[C]_t = [A]_0 \left\{1 + \frac{k_2 e^{-k_1 t} - k_1 e^{-k_2 t}}{k_2 - k_1}\right\}. \quad (15)$$

These equations allow a good description of the hydrogenated fiber behavior under insolation of 244 nm UV. Considering that the emission intensity around 400 nm is proportional to the number of GLPCs, so of species B, the equation (11) allows, as shown in Figure 2, a good adjustment of the signal. This model also makes it possible to account also for the behavior of the non-hydrogenated fiber. As previously reported, GLPCs exist in germanosilicate fibers prior to any treatment and can also be created in the absence of hydrogen [12]. Taking into account that the kinetics of their transformation is much slower than in the presence of hydrogen, which makes it necessary to consider that the concentration of the species B is not null at the initial moment, this model leads at a good signal adjustment around 400 nm (Figure 2). It can be pointed out at this level that the adjustment without taking into account the possibility of creating GLPCs during sunstroke does not make it possible to correctly reproduce the observed evolution. Figure 3 shows the evolution of the signal around 400 nm as a function of time. Single-exponential fit tests do not describe the signal over the duration of the follow-up.

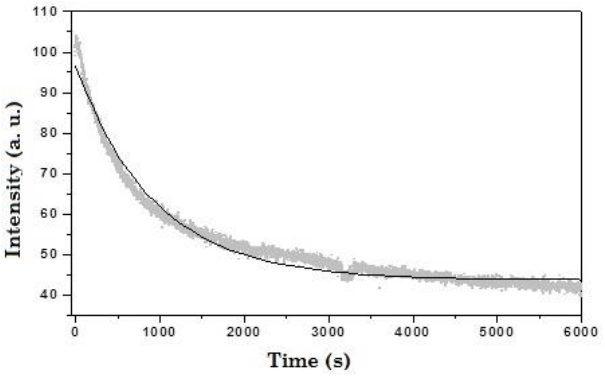

Fig. 3 – Evolution of emission around 400 nm of the non-hydrogenated fiber during 244 nm insolation with the spherical lens, full line: fit with an exponential

Moreover, as mentioned before, the kinetics of formation and transformation of GLPCs clearly show a dependence as a function of insolation energy density [8, 12]. To determine this dependence, the same fiber was subjected to different powers and our spectra were recorded for times up to about 5000 seconds. From one experiment to another, the point of "focusing" of the incident UV beam was changed by moving the fiber about ten centimeters in the opposite direction to the detection. Figure 4 shows the time evolution of this signal under 40, 30, and 20 mW of insolation power. Although the overall behavior remains the same, the associated kinetics are different.

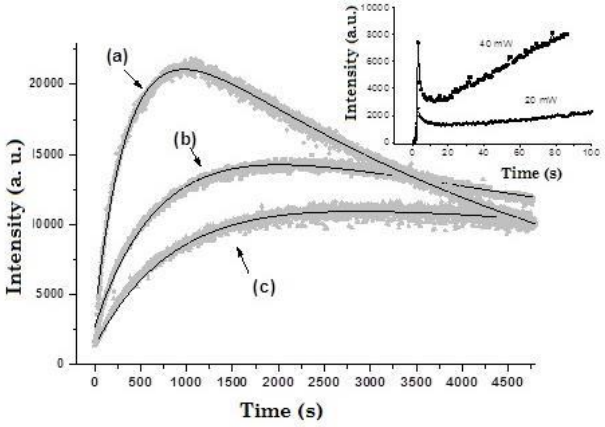

Fig. 4 – Temporal evolution of the signal around 400 nm of a hydrogenated fiber under different UV insolation powers: (a) 40 mW, (b) 30 mW and (c) 20 mW. The solid lines correspond to the adjustment obtained via the proposed model. Inset: Evolution of emission for short times

The use of the relation (11) for performing the adjustments allows the determination of the constants k_1 and k_2 and the monitoring of their variation as a function of the laser power used for the insolation. Figure 5 gives the evolution of k_1 and k_2 as a function of this power. Note that, on the power range studied, the latter follow an exponential evolution. Note that for relatively short times, the signal around 400 nm first begins to decrease before the trend reverses as shown in the inset in Figure 4.

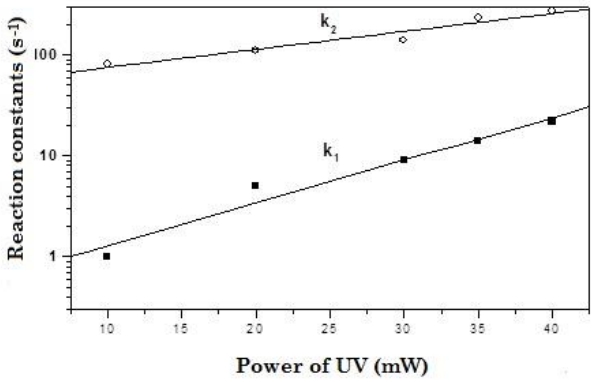

Fig. 5 – Evolution of the kinetics of formation and destruction of the defects emitting around 400 nm according to the power of insolation

The results presented Figure 5 are the result of the direct recording of the signal around 400 nm. They do not take into account the effect that UV insolation may have on the propagation properties of light around 400 nm. It have been studied the modification of the transmission in the presence of the UV insolation field: photo-darkening or "photodarkening" [13]. This effect can alter the signal propagated in the fiber and distort the perception of its temporal evolution. They have shown that photo-darkening can, in some cases, significantly alter the propagated signal. Under these conditions, they suggested collecting light emitted transversely (from the side) and not at the end of fiber because in this case the path traveled would be shorter.

To evaluate the influence of photo-darkening on our measurements, we injected into the fiber a low-power laser beam at 488 nm and we followed the evolution of the intensity transmitted in the presence and absence of UV insolation. This experiment has shown that insolation, even at a UV power (≈ 70 mW) higher than that used in our studies, does not modify the temporal behavior of the transmission of the fiber (during the duration of the insolation). While it is true that the presence or absence of UV radiation induces a variation of a few percent of the transmission (Figure 6), it remains almost constant as long as the external stresses do not change. As a result, the evolution as a function of time of the signal around 400 nm, observed even over a few seconds, can not be attributed to a photo-darkening effect and is therefore due to an evolution of the transmitting centers.

The model described and applied for the previous explanation of the evolution of the signal around 400 nm considers that the species created is the same as the destroyed species but with creation kinetics much lower than that of their destruction. If the GLPC defects are at the origin of the emission at 400 nm, it remains, however, to be complete, to determine the precursor *A* and the result *C* of the transformation of these defects. It proposed, based on different experimental studies [11-12],

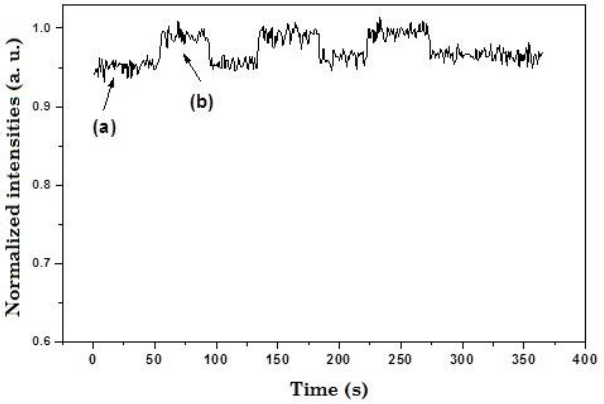

Fig. 6 – Evolution of the transmission at 488 nm in a virgin fiber: (a) without UV insolation, (b) under lateral insolation (70 mW at 244 nm)

that species *B* is, if not originally, at least related to absorption at 240 nm. Without specifying the precursor A, it states that the transformation, of this species B, involves the formation of Ge-H and that the species C, final product of the transformation, is most probably a defect GeE '. These different hypotheses [13-14] are not in contradiction with our experimental observations. Indeed, the GLPCs admit an absorption band around 240 nm which allows the excitation of the level S1 and their transformation, as we have seen, goes well with the formation of Ge-H. This formation of Ge-H was confirmed by Raman scattering both under insolation at 244 and 325 nm. Moreover, the rupture of a Ge-Si or Ge-Ge bond of an ODC defect does not exclude the formation of a defect GeE' [15]. The latter is not optically active and cannot, therefore, follow its evolution by emission spectroscopy.

Despite these concordances and the convergences between our observations, the mechanisms described above should not be the only ones involved. It is even possible that the formation of GLPCs from a precursor A does not constitute the main 'feedback' channel of the emission around 400 nm during the insolation.

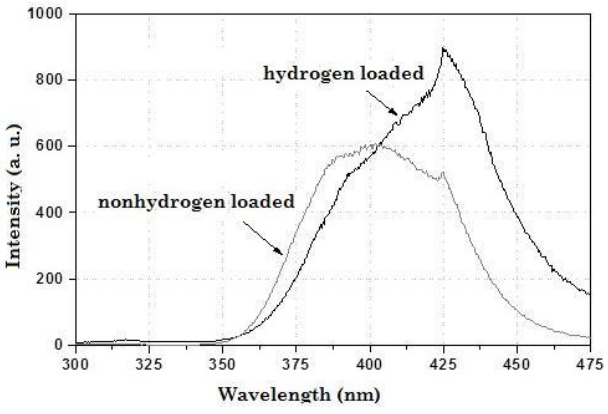

Fig. 7 – Luminesence spectrum of hydrogenated and non-hydrogenated fibers after 500 s insolation at 244 nm and 60 mW of laser power

It can be remembered at this level that the emission profile around 400 nm has been modified during the insolation at 325 nm. The modification, as explained above, may be due to a multiple contribution to this issue.

The same phenomenon was observed during the insolation at 244 nm. As shown in Figure 7, the emission profile at 400 nm, both in the case of the non-hydrogenated fiber and the hydrogenated fiber, was affected by insolation at 244 nm. In the latter case, the change is substantial. The two spectra of this figure were recorded by lowering, after 500 seconds of insolation, the power of the laser so that the evolution during the recording is as slow as possible. These spectra show the appearance of a 425 nm component whose contribution to the signal around 400 nm is not negligible, especially in the case of the hydrogenated fiber. This component is completely absent from the virgin fiber spectrum and is the result, in this case, of the exposure of the fiber to UV radiation. However, in the general case, its appearance should not be exclusively the result of exposure to UV radiation.

4. CONCLUSIONS

The emission evolution at 400 nm is discussed as part of a two-stage transformation of the transmitting centers. The results showed that this model does not make it possible to account for all of our experimental observations. In the light of this discussion, we propose the various transformation stages of the transmitting centers around 400 nm. Kinetics the creation of defects in the hydrogenated fiber follows the power law for low-fluence insolation. At high fluency the formation of defects follows the principle of two photosensitization or serial steps.

REFERENCES

1. H.N. Li, D.S. Li, G.B. Song, *Eng. Struct.* **26** (11), 1647 (2004).
2. Y. Quiquempois, P. Niay, M. Douay, B. Poumelec, *Cur. Opin. Sol. Sta. Mat. Sci.* **7** (2), 89 (2003).
3. M. Lancry, P. Niay, S. Bailleux, M. Douay, C. Depecker, P. Cordier, I. Riant, *Appl. Opt.* **41**(34),7197 (2002).
4. L. Paccou, M. Lancry, M. Douay, *Opt. Expr.* 13, 7342 (2005).
5. A. Alessi, S. Girard, M. Cannas, S. Agnello, A. Boukenter, Y. Ouerdane, *Opt. Expr.* **19**, 11680 (2011).
6. L. Giacomazzi, L. Martin-Samos, A. Boukenter, Y. Ouerdane, S. Girard, N. Richard, *Opt. Mat. Expr.* **5** (5), 1054 (2015).
7. J. Canning, H.J. Deyerl, H.R. Sorensen, M. Kristensen, *J. Appl. Phys.* **97** (5), 053104 (2005).
8. X. Zhang, L. Shao, H. He, W. Pan, L. Yan, *Appl. Opt.* **56**, 6201 (2017).
9. J. Canning, *Proc. SPIE* **7004**, 700409 (2008).
10. F. Messina, M. Cannas, K. Medjahdi, A. Boukenter, Y. Ouerdane, *Proc. WOPC* (2015).
11. P. Jiang, W. Bi, Y. Qi, Y. Wu, F. Wang, P. Tian, *Opt.* **127** (11), 4605 (2016).
12. R. Wang, J. Si, T. Chen, L. Yan, H. Cao, X. Pham, X. Hou, *Opt. Expr.* **25**, 23684 (2017).
13. M. Shaimerdenova, A. Bekmurzayeva, M. Sypabekova, D. Tosi, *Opt. Expr.* **25**, 33487 (2017).
14. C. Marciniak, H. Ball, A. Hung, M. Biercuk, *Opt. Exp.* **25**, 15643 (2017).
15. G. Simpson, K. Kalli, J. Canning, A. Lacraz. *Proc. BGPP BTh3B.4* (2016).